

Article

Generation of Pre-Caldera Qixiangzhan and Syn-Caldera Millennium Rhyolites from Changbaishan Volcano by Shallow Remelting: Evidence from Zircon Hf–O Isotopes

Haibo Zou ^{1,*}  and Jie Tong ²¹ Department of Geosciences, Auburn University, Auburn, AL 36849, USA² State Key Laboratory of Continental Dynamics, Department of Geology, Northwest University, Xi'an 710069, China; tongjie0880@163.com

* Correspondence: haibo.zou@auburn.edu

Abstract: The Changbaishan volcano is well known for its major caldera-forming Millennium Eruption (ME) in 946 CE (Common Era). We report Hf–O isotopes of zircon grains from pre-caldera Qixiangzhan (QXZ) and syn-caldera eruptions of the Changbaishan (Baitoushan) volcano to constrain magma chamber processes. Zircon grains from the pre-caldera QXZ comendite lavas have $\delta^{18}\text{O}$ ranging from 4.46 to 5.16 (lower than mantle values) and ϵ_{Hf} ranging from -4.47 to $+4.37$. Zircon grains from the syn-caldera ME1 charcoal-bearing non-welded comendite pyroclastic flow deposits have $\delta^{18}\text{O}$ ranging from 2.25 (lower than mantle values) to 5.51 and ϵ_{Hf} from -3.75 to $+3.31$. By comparison, zircon grains from the ME2 welded trachytes have $\delta^{18}\text{O}$ ranging from 5.66 to 6.20 (higher than mantle zircon values) and ϵ_{Hf} from -1.97 to $+6.23$. There are no correlations between O and Hf isotopes for all zircon grains in QXZ and ME1 comendites and ME2 trachyte. The ubiquitous occurrence of low- $\delta^{18}\text{O}$ zircon grains in QXZ and ME1 comendites indicates shallow remelting of hydrothermally altered low- $\delta^{18}\text{O}$ juvenile rocks. By contrast, ME2 trachyte zircons (except for two zircon grains) have normal $\delta^{18}\text{O}$ (5.66 to 6.10) values, indicating a lack of remelting processes. Similar zircon Hf–O isotopes between pre-caldera QXZ comendites and syn-caldera ME1 comendites indicate tapping of the upper portion of a zoned magma chamber. Higher $\delta^{18}\text{O}$ in ME2 trachyte zircons indicate tapping of the deeper portion of a zoned magma chamber free from shallow remelting. The lack of significant correlations between zircon O and Hf isotopes, and the relatively high ϵ_{Hf} values for all Changbai zircon grains, argue against partial melting of ancient continental crust or significant contaminations by ancient crustal rocks as an origin for these felsic magmas. The QXZ and ME1 comendites were formed by shallow remelting of hydrothermally altered juvenile volcanic rocks, and ME2 trachytes were formed by evolution of mantle-derived basaltic magmas free of hydrothermal assimilations. A proto-caldera likely formed prior to the generation of QXZ lavas at 10 ka.

Keywords: Changbaishan (Baitoushan) volcano; comendite; trachyte; zircon Hf–O isotopes; zoned magma chamber; Qixiangzhan (QXZ) lava; Millenium Eruption



Citation: Zou, H.; Tong, J. Generation of Pre-Caldera Qixiangzhan and Syn-Caldera Millennium Rhyolites from Changbaishan Volcano by Shallow Remelting: Evidence from Zircon Hf–O Isotopes. *Minerals* **2024**, *14*, 1297. <https://doi.org/10.3390/min14121297>

Academic Editors: Benigno E. Godoy, Petrus J Le Roux, Inés Rodríguez and Marco Taussi

Received: 11 November 2024

Revised: 11 December 2024

Accepted: 19 December 2024

Published: 22 December 2024



Copyright: © 2024 by the authors. Licensee MDPI, Basel, Switzerland. This article is an open access article distributed under the terms and conditions of the Creative Commons Attribution (CC BY) license (<https://creativecommons.org/licenses/by/4.0/>).

1. Introduction

The caldera-forming Millenium Eruption (ME) in 946 CE (Common Era) of the Changbaishan (Baitoushan) volcano [1–6] on the China–North Korea border (Figure 1) is one of the two largest eruptions on Earth over the past 1100 years and produced early-stage comendites (ME1) and late-stage trachytes (ME2). Prior to the ME, the pre-caldera Qixiangzhan (QXZ) eruption of peralkaline rhyolites took place at ~10 ka [7,8]. After the ME, one or more small eruptions occurred in the past 300 years [9], including the post-caldera 0.3 ka Baguamiao eruption [7,9]. A stagnant Pacific slab is present beneath northeast Asia [10], and Changbaishan is located in a Cenozoic rift system that formed as a response to the subduction of the western Pacific beneath northeast Asia [6].

Magnetic excursion was discovered in the QXZ lava and may represent the youngest magnetic excursion on Earth [11]. Earlier reported ages of the QXZ range from 17.1 ± 0.9 ka by sanidine Ar/Ar [11] to 12.2 ± 1.7 ka by zircon U-series [7]. Recent Ar/Ar dating of sanidine yielded an age of 10.2 ± 0.8 ka [8], which is more consistent with the zircon U-series age for QXZ reported by Zou et al. [7].

Zircon U-series ages for the QXZ, ME, and Baguamiao eruptions at the Changbaishan volcano have been reported [1,7,12,13]. Zircon age populations are 12 ka for QXZ zircons, 1 ka, 10 ka, and 100 ka for ME zircons, and 2 ka and 100 ka for Baguamiao zircons.

It has been demonstrated that igneous zircon Hf–O isotopes are powerful for determining magmatic processes and sources [14–18]. Although some zircon Hf–O isotopes have been reported for Millennium eruptions [19,20], these ME samples came from the north slope of Changbaishan. ME eruptions, including ME1 charcoal-bearing pyroclastic flows, were significantly better exposed on the southern side than the northern side [9]. In addition, zircon Hf–O isotopes from the pre-caldera QXZ eruption and ME2 trachyte remain to be analyzed.

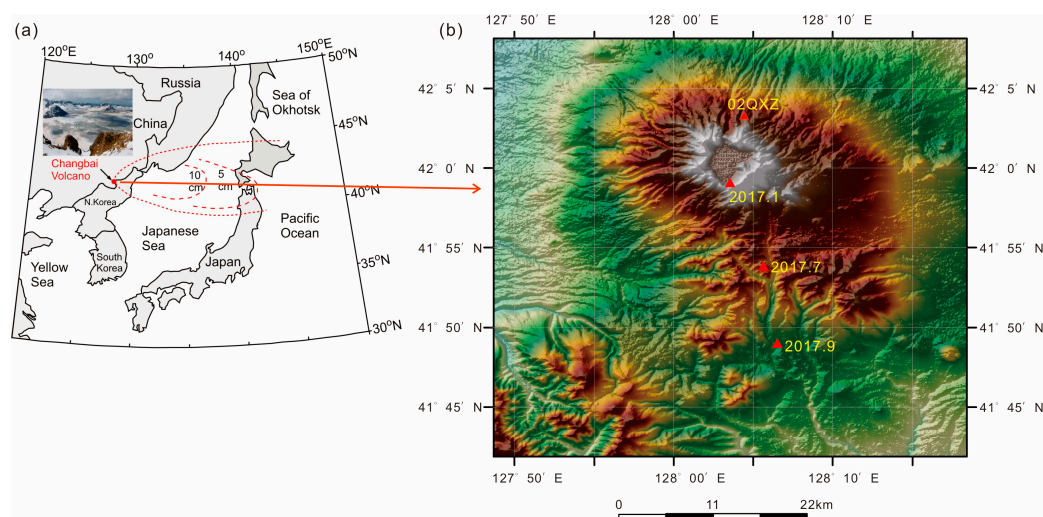


Figure 1. (a) Location of the Changbaishan volcano between the China–North Korea border. The 5 cm and 10 cm dashed lines represent the thickness of volcanic ash deposits [21]. (b) Sample locations from the Changbaishan volcano. ME2 sample 2017.7 (N $41^{\circ}53'38.66''$, E $128^{\circ}05'47.22''$) and ME1 sample 2017.9 (N $41^{\circ}48'49.56''$, E $128^{\circ}06'38.80''$) are located on the south slope of the Changbaishan volcano. 02QXZ is located on the north slope of the Changbaishan volcano. Revised after Zou et al. [12].

This Hf–O isotope study was first presented as an abstract for the 2023 Goldschmidt Conference [22]. This paper provides details for Changbaishan zircons. Here, we report low- $\delta^{18}\text{O}$ zircons for pre-caldera QXZ comendites and normal $\delta^{18}\text{O}$ oxygen zircons in ME2 trachytes. Our new zircon Hf–O data for ME1 comendites are compared with previous results. More importantly, comparisons of Hf–O isotopes in QXZ and ME2 zircons with those of ME1 zircons provide new insights into the magma chamber processes for the Changbaishan volcano.

2. Materials and Methods

QXZ comendite lavas are porphyritic. Phenocrysts include sanidine, hedenbergite, and fayalite, and groundmass includes glass and sodic amphibole [7]. ME1 comendites are composed of glass and unzoned phenocrysts of sanidine, hedenbergite, and fayalite. ME2 trachytes are composed of glasses and phenocrysts of anorthoclase, hedenbergite, and fayalite [12].

Rock samples from the Changbaishan volcano were crushed into a 40–60 mesh in agate mortars. Zircons were separated carefully under a microscope. Representative zircon

grains were mounted on epoxy resin disks. Cathodoluminescence (CL) images were used to characterize the internal structures of the zircon grains.

Zircon oxygen isotopic compositions were measured using a CAMECA IMS-1280HR ion microprobe at the Institute of Geology and Geophysics, Chinese Academy of Sciences. A 2 nA Cs⁺ primary beam was focused onto a 20–30- μ m-diameter oval spot. Secondary ions were accelerated at 10 keV. Detailed analytical methods have been documented in Li et al. [23]. Penglai zircon [24] was used as the external standard for oxygen isotope analyses.

Zircon Hf isotopic compositions were measured using a Thermo Finnigan Neptune MC-ICP-MS at the Institute of Mineral Resources, Chinese Academy of Geological Sciences, with helium as a carrier gas to transport the aerosol. Instrument tuning and data acquisition methods have been documented in Hou et al. [25]. The international zircon standard GJ1 was used as the external standard. Chondrite Hf isotopic compositions [26] are used to calculate zircon ε_{Hf} values.

3. Results

Zircon Hf–O isotope data for QXZ, ME1, and ME2 eruption products are provided in Table 1 and presented in Figure 2. Cathodoluminescence (CL), transmitted light, and reflected light images are provided in Figure 3 for QXZ zircons, Figure 4 for ME1 zircons, and Figure 5 for ME2 zircons.

Table 1. Zircon Hf–O isotopic compositions from Changbaishan volcanic rocks.

Sample	¹⁷⁶ Yb/ ¹⁷⁷ Hf	2SE	¹⁷⁶ Lu/ ¹⁷⁷ Hf	2SE	¹⁷⁶ Hf/ ¹⁷⁷ Hf	2SE	$\varepsilon_{\text{Hf}}(0)$	2 σ	dO ¹⁸	2SE
QXZ02										
02QXZ-02@1	0.109875	0.001501	0.003030	0.000033	0.282798	0.000030	0.93	1.47	4.59	0.35
02QXZ-02@2	0.112778	0.001381	0.002855	0.000027	0.282788	0.000037	0.56	1.66	5.00	0.19
02QXZ-02@3	0.135472	0.000335	0.003210	0.000012	0.282770	0.000035	−0.07	1.61	5.07	0.20
02QXZ-02@4	0.082368	0.000962	0.002173	0.000032	0.282885	0.000047	4.01	1.95	5.16	0.20
02QXZ-02@5	0.157140	0.000601	0.003592	0.000009	0.282896	0.000041	4.37	1.77	4.88	0.15
02QXZ-02@6	0.121092	0.000694	0.003215	0.000014	0.282754	0.000066	−0.63	2.56	4.52	0.13
02QXZ-02@7	0.095148	0.000458	0.002172	0.000004	0.282837	0.000041	2.31	1.78	4.67	0.18
02QXZ-02@8	0.040053	0.000490	0.001044	0.000006	0.282770	0.000039	−0.07	1.73		
02QXZ-02@9	0.130503	0.000557	0.003400	0.000007	0.282872	0.000050	3.55	2.05	4.79	0.19
02QXZ-02@10	0.080459	0.000567	0.002040	0.000008	0.282800	0.000037	0.98	1.66	4.78	0.22
02QXZ-02@11	0.115589	0.000909	0.002743	0.000006	0.282754	0.000049	−0.63	2.02	5.04	0.20
02QXZ-02@12	0.121024	0.000298	0.002879	0.000007	0.282834	0.000033	2.19	1.54	4.87	0.26
02QXZ-02@13	0.047613	0.000120	0.001203	0.000003	0.282725	0.000032	−1.67	1.52	4.94	0.23
02QXZ-02@14	0.094112	0.000372	0.002222	0.000003	0.282646	0.000041	−4.47	1.77	4.69	0.25
02QXZ-02@15	0.115848	0.000215	0.002804	0.000007	0.282748	0.000037	−0.86	1.68	4.83	0.21
02QXZ-02@16	0.067921	0.000375	0.001741	0.000004	0.282693	0.000036	−2.81	1.63	4.92	0.19
02QXZ-02@17	0.109900	0.000159	0.002838	0.000002	0.282771	0.000035	−0.03	1.62	4.46	0.19
02QXZ-02@18	0.088757	0.002044	0.002286	0.000045	0.282862	0.000028	3.18	1.43	4.88	0.22
02QXZ-02@19	0.106776	0.000278	0.002560	0.000017	0.282773	0.000034	0.03	1.59	4.74	0.18
02QXZ-02@20	0.112374	0.000243	0.002648	0.000014	0.282761	0.000039	−0.38	1.73	4.85	0.16
02QXZ-02@21	0.116421	0.000680	0.002718	0.000005	0.282777	0.000035	0.17	1.60	4.66	0.26
02QXZ-02@22	0.116374	0.000337	0.002694	0.000012	0.282724	0.000037	−1.70	1.67	4.67	0.22
02QXZ-02@23	0.115444	0.000248	0.002724	0.000006	0.282731	0.000039	−1.47	1.73	4.81	0.21
02QXZ-02@24	0.121318	0.000487	0.002815	0.000008	0.282821	0.000046	1.74	1.91	4.67	0.18
02QXZ-02@25	0.091317	0.001145	0.002370	0.000035	0.282788	0.000033	0.58	1.56	4.87	0.20
02QXZ-02@26	0.117077	0.000778	0.002729	0.000005	0.282828	0.000055	1.97	2.21	5.00	0.23
02QXZ-02@27	0.117350	0.000625	0.002764	0.000005	0.282835	0.000061	2.23	2.38	4.74	0.14
02QXZ-02@28	0.114655	0.000068	0.002744	0.000012	0.282866	0.000050	3.34	2.03	4.90	0.19
02QXZ-02@29	0.118350	0.000111	0.002684	0.000009	0.282871	0.000073	3.50	2.78	4.98	0.22
02QXZ-02@30	0.110124	0.000356	0.002819	0.000011	0.282789	0.000033	0.59	1.56	4.99	0.28
TCN2019-9 (ME1)										
TCNan-2017-9@1									4.56	0.22
TCNan-2017-9@2	0.068849	0.000330	0.001810	0.000005	0.282839	0.000030	2.36	1.47	4.82	0.18

Table 1. Cont.

Sample	¹⁷⁶ Yb/ ¹⁷⁷ Hf	2SE	¹⁷⁶ Lu/ ¹⁷⁷ Hf	2SE	¹⁷⁶ Hf/ ¹⁷⁷ Hf	2SE	ε _{Hf} (0)	2σ	dO ¹⁸	2SE
TCNan-2017-9@3	0.051259	0.000085	0.001498	0.000004	0.282861	0.000030	3.13	1.47	4.62	0.25
TCNan-2017-9@4	0.049261	0.000120	0.001384	0.000002	0.282811	0.000030	1.38	1.48	4.87	0.21
TCNan-2017-9@5	0.039404	0.000293	0.000991	0.000002	0.282765	0.000033	−0.25	1.55	4.58	0.18
TCNan-2017-9@6	0.101594	0.001062	0.002642	0.000016	0.282790	0.000033	0.62	1.56	4.80	0.19
TCNan-2017-9@7	0.045483	0.000286	0.001363	0.000006	0.282809	0.000045	1.31	1.89	4.65	0.27
TCNan-2017-9@8	0.054058	0.000318	0.001447	0.000012	0.282775	0.000031	0.11	1.50	4.75	0.18
TCNan-2017-9@9	0.041381	0.000282	0.001239	0.000007	0.282854	0.000028	2.89	1.41	5.11	0.18
TCNan-2017-9@10	0.057394	0.000318	0.001893	0.000009	0.282754	0.000034	−0.62	1.59	2.25	0.29
TCNan-2017-9@11	0.046228	0.000328	0.001401	0.000009	0.282832	0.000030	2.14	1.48	4.80	0.15
TCNan-2017-9@12	0.063075	0.000215	0.001819	0.000007	0.282790	0.000030	0.62	1.48	4.83	0.17
TCNan-2017-9@13	0.055606	0.000790	0.001548	0.000024	0.282666	0.000030	−3.75	1.47	5.00	0.19
TCNan-2017-9@14	0.071142	0.000354	0.002034	0.000011	0.282865	0.000033	3.31	1.54	4.70	0.20
TCNan-2017-9@15	0.043023	0.000288	0.001361	0.000008	0.282775	0.000029	0.12	1.46	4.79	0.16
TCNan-2017-9@16	0.049592	0.000662	0.001367	0.000016	0.282714	0.000029	−2.04	1.45	5.15	0.19
TCNan-2017-9@17	0.045210	0.000477	0.001284	0.000011	0.282763	0.000024	−0.30	1.33	4.92	0.19
TCNan-2017-9@18	0.037986	0.000164	0.001231	0.000006	0.282809	0.000031	1.32	1.51	4.80	0.23
TCNan-2017-9@19	0.028984	0.000088	0.000843	0.000003	0.282725	0.000029	−1.65	1.46	5.08	0.22
TCNan-2017-9@20	0.054602	0.000424	0.001640	0.000011	0.282826	0.000028	1.90	1.44	5.28	0.22
TCNan-2017-9@21	0.037966	0.000536	0.001143	0.000014	0.282809	0.000032	1.30	1.52	4.91	0.18
TCNan-2017-9@22	0.065069	0.000258	0.001964	0.000007	0.282802	0.000038	1.06	1.70	4.62	0.19
TCNan-2017-9@23	0.052940	0.000481	0.001650	0.000012	0.282783	0.000033	0.38	1.56	5.05	0.23
TCNan-2017-9@24	0.073384	0.000280	0.002188	0.000012	0.282677	0.000044	−3.34	1.87	5.06	0.21
TCNan-2017-9@25	0.036474	0.000594	0.001110	0.000018	0.282845	0.000029	2.57	1.45	5.51	0.54
TCN2017-7 (ME2)										
TCNan2017-7@1	0.064156	0.000376	0.001805	0.000005	0.282821	0.000032	1.74	1.52	5.91	0.33
TCNan2017-7@2	0.046074	0.000034	0.001253	0.000004	0.282789	0.000028	0.60	1.43	5.84	0.20
TCNan2017-7@3	0.049470	0.000165	0.001487	0.000001	0.282796	0.000031	0.86	1.50	5.78	0.23
TCNan2017-7@4	0.041150	0.000225	0.001278	0.000003	0.282859	0.000033	3.09	1.55	5.98	0.25
TCNan2017-7@5	0.094709	0.000290	0.002723	0.000004	0.282862	0.000030	3.20	1.47	5.95	0.23
TCNan2017-7@6	0.100152	0.000458	0.002921	0.000006	0.282808	0.000031	1.28	1.50	5.87	0.23
TCNan2017-7@7	0.107003	0.000490	0.003109	0.000005	0.282749	0.000031	−0.81	1.50	5.78	0.17
TCNan2017-7@8	0.059984	0.000410	0.001974	0.000015	0.282805	0.000034	1.18	1.58	6.10	0.30
TCNan2017-7@9	0.115905	0.001021	0.003294	0.000019	0.282732	0.000033	−1.41	1.56	5.87	0.17
TCNan2017-7@10	0.078112	0.000620	0.002313	0.000013	0.282850	0.000031	2.76	1.50	5.88	0.21
TCNan2017-7@11	0.101072	0.001351	0.002687	0.000033	0.282834	0.000034	2.18	1.59	5.83	0.20
TCNan2017-7@12	0.107792	0.000943	0.003047	0.000019	0.282829	0.000037	2.01	1.66	5.97	0.19
TCNan2017-7@13	0.069185	0.000425	0.001934	0.000017	0.282744	0.000036	−0.98	1.63	5.96	0.19
TCNan2017-7@14	0.081124	0.000183	0.002309	0.000002	0.282914	0.000045	5.02	1.88	6.10	0.20
TCNan2017-7@15	0.074576	0.000215	0.002004	0.000008	0.282748	0.000031	−0.84	1.49	5.79	0.15
TCNan2017-7@16	0.082377	0.000681	0.002468	0.000016	0.282871	0.000030	3.52	1.48	5.88	0.19
TCNan2017-7@17	0.076482	0.000353	0.002569	0.000012	0.282875	0.000045	3.65	1.90	3.56	1.89
TCNan2017-7@18	0.062085	0.000330	0.001839	0.000005	0.282771	0.000037	−0.04	1.67	6.04	0.20
TCNan2017-7@19	0.080927	0.000504	0.002472	0.000024	0.282875	0.000040	3.65	1.75	5.82	0.17
TCNan2017-7@20	0.057417	0.000547	0.001653	0.000008	0.282874	0.000059	3.60	2.32	6.04	0.21
TCNan2017-7@21	0.040722	0.000256	0.001396	0.000005	0.282768	0.000034	−0.14	1.59	6.02	0.23
TCNan2017-7@22	0.099720	0.001199	0.002918	0.000028	0.282824	0.000028	1.85	1.43	5.83	0.21
TCNan2017-7@23	0.041053	0.000255	0.001466	0.000007	0.282747	0.000036	−0.88	1.63	6.07	0.17
TCNan2017-7@24	0.078873	0.000143	0.002264	0.000010	0.282813	0.000031	1.44	1.51	5.93	0.21
TCNan2017-7@25	0.108831	0.001245	0.003455	0.000034	0.282716	0.000031	−1.97	1.49	5.80	0.22
TCNan2017-7@26									1.68	0.27
TCNan2017-7@27	0.109531	0.000290	0.003631	0.000008	0.282786	0.000042	0.50	1.81	5.66	0.21
TCNan2017-7@28	0.057431	0.000286	0.001899	0.000008	0.282834	0.000029	2.20	1.46	5.89	0.21
TCNan2017-7@29	0.102275	0.001089	0.002865	0.000025	0.282948	0.000033	6.23	1.56	4.81	0.17
TCNan2017-7@30	0.083293	0.000215	0.002536	0.000004	0.282900	0.000033	4.52	1.55	5.89	0.27
TCNan2017-7@31	0.046286	0.000123	0.001680	0.000004	0.282739	0.000033	−1.17	1.56	6.12	0.25
TCNan2017-7@32	0.040661	0.000214	0.001492	0.000010	0.282737	0.000034	−1.23	1.59	6.20	0.21
TCNan2017-7@33	0.121413	0.000809	0.004071	0.000030	0.282790	0.000041	0.65	1.78	6.06	0.19
TCNan2017-7@34	0.120128	0.000073	0.003816	0.000003	0.282883	0.000030	3.94	1.47	6.04	0.18
TCNan2017-7@35									6.20	0.27

Zircon grains from the Qixiangzhan (QXZ) comendite lavas on the northern slope of the Changbai volcano have $\delta^{18}\text{O}$ ranging from 4.46 to 5.16 and ϵ_{Hf} ranging from -4.47 to $+4.37$. Their $\delta^{18}\text{O}$ values are lower than the mantle zircon values of 5.3 ± 0.3 [27].

Zircon grains from the ME1 charcoal-bearing non-welded comendite pyroclastic flow deposit on the southern slope of the Changbaishan volcano have $\delta^{18}\text{O}$ ranging from 2.25 to 5.51 and ϵ_{Hf} from -3.75 to $+3.31$. Their $\delta^{18}\text{O}$ values are also lower than the mantle zircon values of 5.3 ± 0.3 . Our zircon Hf–O isotope data for ME1 comendites are in agreement with the zircons reported for ME zircons from the northern side [19,20].

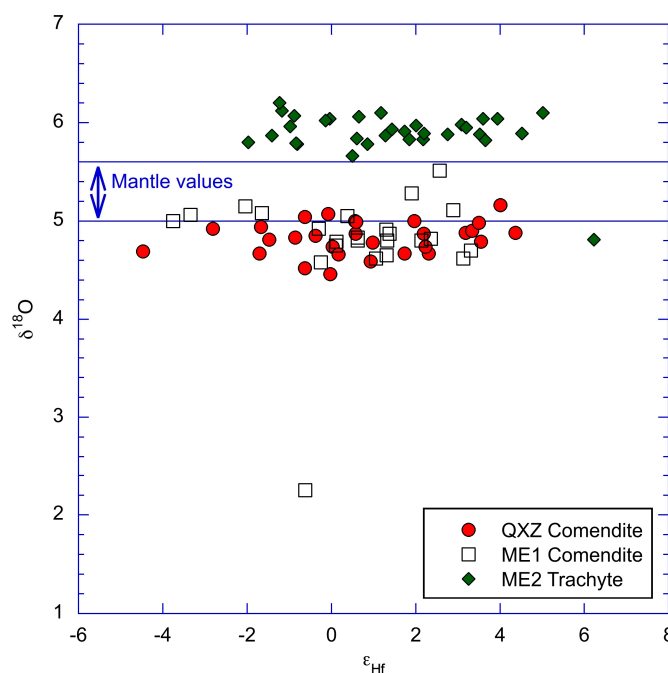


Figure 2. Zircon Hf–O isotopes for pre-caldera QXZ lavas, ME1 non-welded charcoal bearing pyroclastic flow deposits, and ME2 welded trachyte pyroclastic flow deposits. Note the low $\delta^{18}\text{O}$ for zircons from QXZ comendites and the ME1 comenditic non-welded pyroclastic flow deposit.

In comparison, most zircon grains from ME2 welded trachytes on its southern slope have $\delta^{18}\text{O}$ ranging from 5.66 to 6.20 (higher than mantle values) and ϵ_{Hf} from -1.97 to $+6.23$. One zircon has $\delta^{18}\text{O}$ of 4.81, similar to the QXZ and ME zircons. One zircon has $\delta^{18}\text{O}$ of 3.56, but this zircon has a large error (Table 1) and is not plotted. The third zircon has very low $\delta^{18}\text{O}$ of 1.68. This zircon does not have Hf isotope data and thus is not plotted in Figure 3.

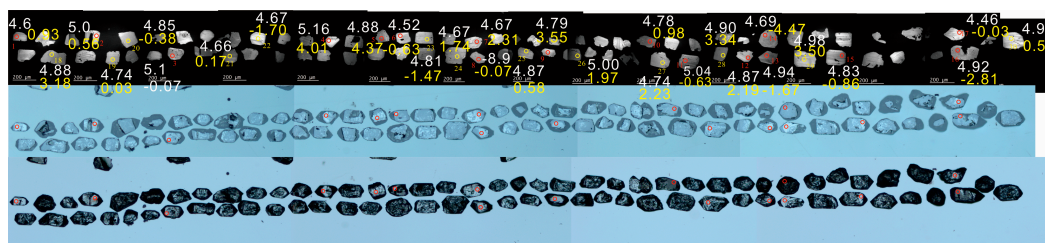


Figure 3. Pre-caldera QXZ zircon CL images (top), transmitted light images (middle), and reflected light images (bottom). The white real numbers are oxygen isotope compositions in $\delta^{18}\text{O}$; the yellow real numbers are Hf isotopic compositions in ϵ_{Hf} . Circles represent analysis spots. The integers (e.g., 1, 2) represent spot numbers.

There are no correlations between O and Hf isotopes for all zircon grains from QXZ, ME1 comendites and ME2 trachyte (Figure 2).

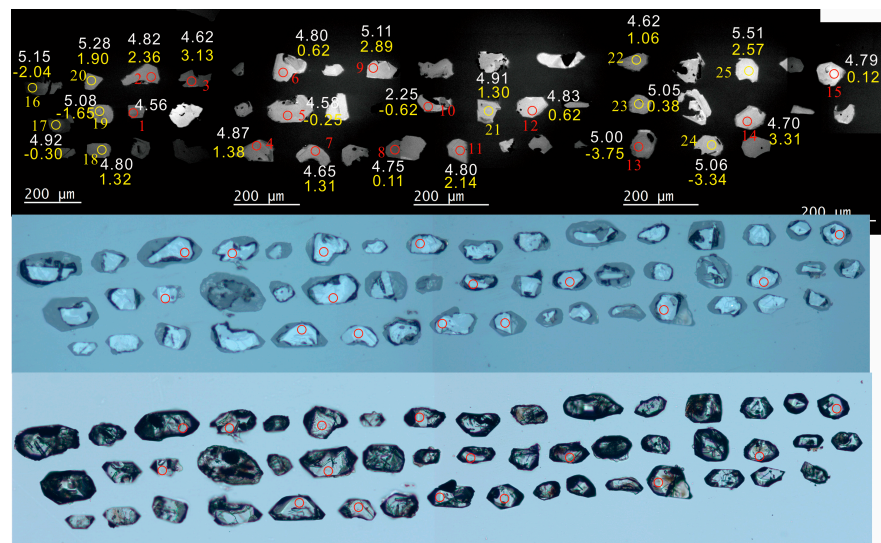


Figure 4. ME1 (sample 2017.9) zircon CL images (**top**), transmitted light images (**middle**), and reflected light images (**bottom**). The white real numbers are oxygen isotope compositions in $\delta^{18}\text{O}$; the yellow real numbers are Hf isotopic compositions in ϵ_{Hf} . Circles represent analysis spots. The integers (e.g., 1, 2) represent spot numbers.

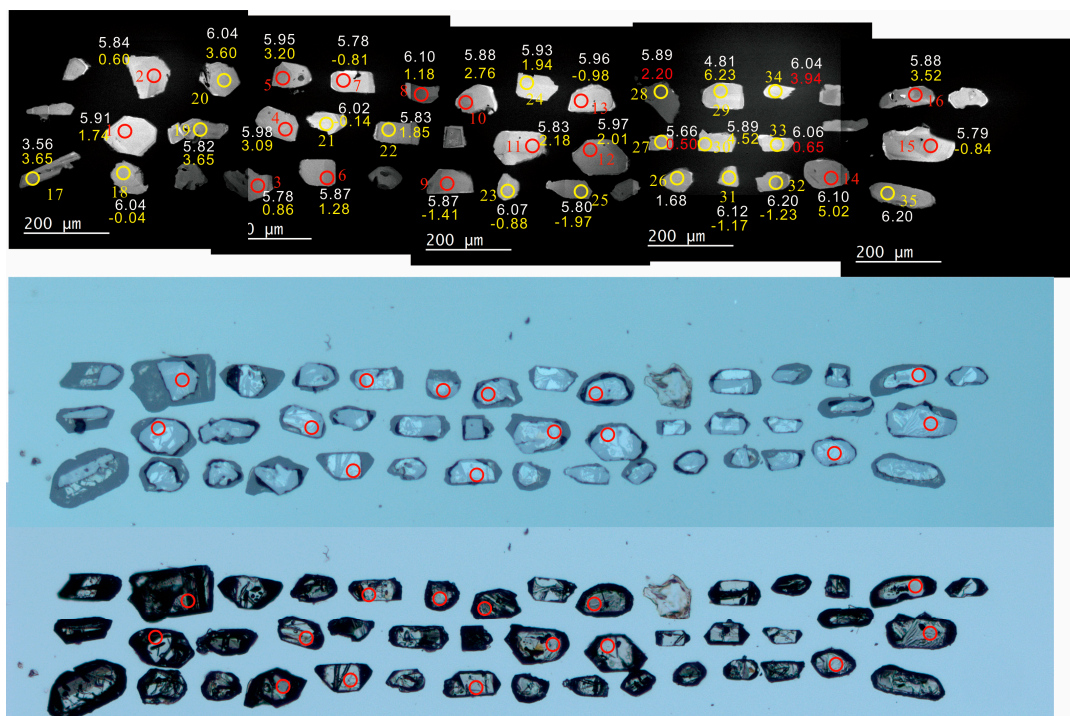


Figure 5. ME2 (sample 2017.7) zircon CL images (**top**), transmitted light images (**middle**), and reflected light images (**bottom**). The white real numbers are oxygen isotope compositions in $\delta^{18}\text{O}$; the yellow real numbers are Hf isotopic compositions in ϵ_{Hf} . Circles represent analysis spots. The integers (e.g., 1, 2) represent spot numbers.

4. Discussion

4.1. Low- $\delta^{18}\text{O}$ Zircons in QXZ and ME1 Comendites by Shallow Remelting

Earlier studies have shown that ME zircons from the north slope of the Changbaishan volcano have low $\delta^{18}\text{O}$ values relative to mantle zircon $\delta^{18}\text{O}$ values. Our ME data from the south slope reveal similarly low- $\delta^{18}\text{O}$ zircons in ME1 comendites (Figure 6) but normal

zircons in ME2 trachytes. We further show that pre-caldera QXZ zircons also have low $\delta^{18}\text{O}$ values, similar to the ME1 comendites.

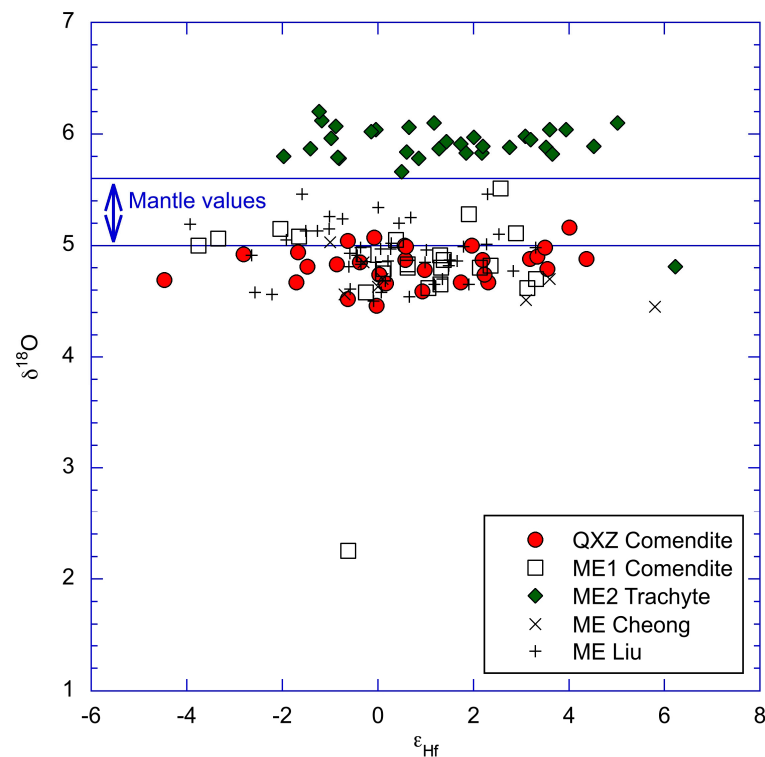


Figure 6. Comparison of ME zircons from this study (open square) and previous data (x, ME Cheong [13]; +, ME Liu [20]). All three studies yield similar ME zircon Hf–O isotope data.

Low- $\delta^{18}\text{O}$ zircons in volcanic rocks may indicate the assimilation or remelting of hydrothermally altered low- $\delta^{18}\text{O}$ juvenile rocks [28–32]. The ubiquitous occurrence of low- $\delta^{18}\text{O}$ zircons in QXZ comendite lava and ME1 charcoal-bearing comendites indicates shallow remelting of hydrothermally altered low- $\delta^{18}\text{O}$ juvenile rocks in the Changbaishan magma chamber.

The occurrence of low- $\delta^{18}\text{O}$ zircons in pre-caldera QXZ zircons suggests that the shallow remelting process occurred earlier than the eruption age of QXZ at 10 ka. Similar zircon Hf–O isotopes between QXZ comendites and ME1 comendites suggest tapping of the same shallow magma chamber.

If a caldera collapse is often needed for the generation of low- $\delta^{18}\text{O}$ rhyolites, then the occurrence of low- $\delta^{18}\text{O}$ zircons in the pre-caldera QXZ lavas may indicate that an earlier proto-caldera might have existed before the eruption of the 10 ka QXZ lavas, significantly prior to the ME eruption in 946 CE. The proto-caldera might have formed during the eruption of the Yellow Pumice at the northern rim.

The depth of shallow remelting can be estimated from the present-day magma chamber depth. The depth of the current magma chamber has been estimated as 4 to 8 km [33–37]. It has been demonstrated that surface waters may penetrate to a depth of 8–10 km in the caldera or rift zone extensional setting [38]. Thus, the shallow depth of the Changbaishan magma chamber provide ideal conditions to form low- $\delta^{18}\text{O}$ QXZ and ME1 comendites.

Although deep melting of subducted oceanic crust that has interacted with seawater at high temperature can generate low- $\delta^{18}\text{O}$ magmas [39–41] and can explain the genesis of Quaternary low- $\delta^{18}\text{O}$ magmas in East Sea (Sea of Japan) [17], we prefer shallow remelting of early formed volcanic rocks for Changbaishan QXZ and ME1 rocks, as the less evolved ME2 trachytes show normal $\delta^{18}\text{O}$ signatures (next section).

4.2. Normal- $\delta^{18}\text{O}$ Zircons in ME2 Trachytes at a Deeper Level

Zircon grains from ME2 trachytes (sample 2017.7) have $\delta^{18}\text{O}$ values between 5.6 and 6.2, slightly higher than mantle zircon values at 5.3 ± 0.3 (Figure 5). The dominant presence of normal- $\delta^{18}\text{O}$ zircons in the ME2 trachytes indicate that the ME2 trachytes were not affected by shallow remelting processes, unlike the ME1 zircons for Changbaishan.

This is consistent with the generation of ME2 trachytes at a greater depth than QXZ comendites and ME1 comendites [12]. Higher $\delta^{18}\text{O}$ values in trachyte zircons indicate tapping of the deeper portion of a zoned magma chamber or a separate deeper magma chamber (Figure 7). The depth of the trachyte magma chamber below Changbaishan is estimated as 13–30 km [34], likely beyond the reach of surface water penetrations at Changbaishan (Figure 7). The ME2 trachytes were formed by differentiation of mantle-derived basaltic magmas under reducing conditions [12].

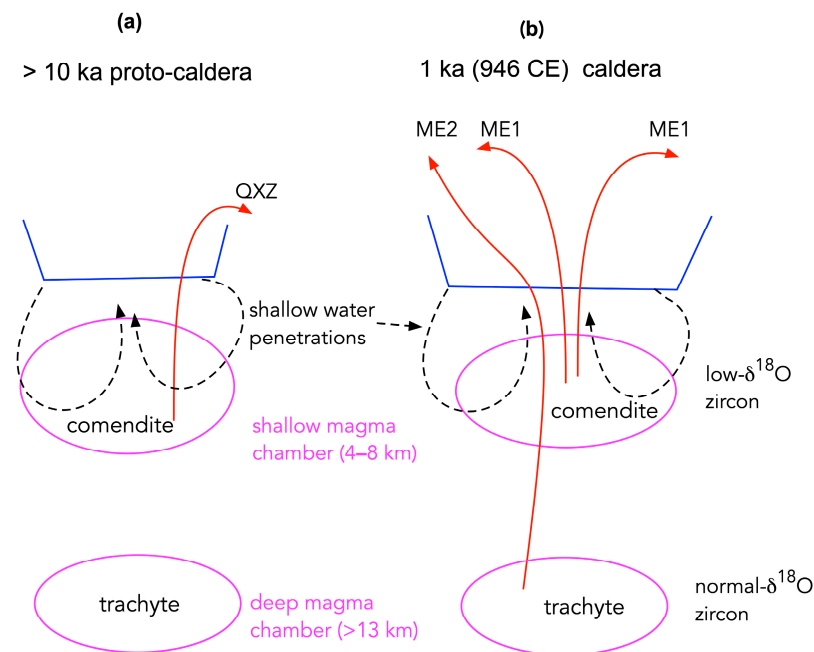


Figure 7. (a) Proto-caldera prior to 10 ka and (b) mature caldera in 946 CE for the Changbaishan volcano. Low- $\delta^{18}\text{O}$ zircons formed in the shallow magma chamber rather than the deep magma chamber.

Despite different oxygen isotope compositions between comendites and trachytes, their ranges of Hafnium isotopic compositions are very similar. This is because oxygen isotopes are sensitive to surface water–rock interactions, whereas hafnium isotopes are not affected by surface water interactions.

4.3. Lack of Hf–O Isotope Correlations for Changbaishan Zircons

QXZ, ME1, and ME2 zircon grains do not show any significant correlations between zircon O and Hf isotopes. This contrasts with the negative zircon Hf–O isotope correlations for Tengchong volcanics from the SE Tibetan Plateau [14,15], where magma contaminations by country rocks took place (Figure 8). The lack of Hf–O isotope correlations and the relatively high ϵ_{Hf} values for all Changbaishan zircons argue against partial melting of ancient continental crust as an origin for these felsic magmas.

Although we do not have Hf isotope compositions for the whole rocks in this paper, we have Hf isotope compositions for similar rocks from Changbaishan. Their whole-rock $^{176}\text{Hf}/^{177}\text{Hf}$ values are 0.282776 ± 4 for P-2 (ME1 comendite) and 0.272779 ± 3 for P-4 (ME2 trachyte). Thus, their ϵ_{Hf} values are 0.15 for P-2 and 0.23 for P-4, similar to the chondritic values. Note that their ϵ_{Nd} values are also close to the chondritic values: -1.1

for P-2 and -1.0 for P-4 [42]. Whole-rock Hf-Nd isotopes for ME1 comendites and ME2 trachytes resemble each other and are similar to the chondritic values. These chondritic Hf-Nd values for Changbaishan felsic magmas also argue against partial melting of ancient continental crust.

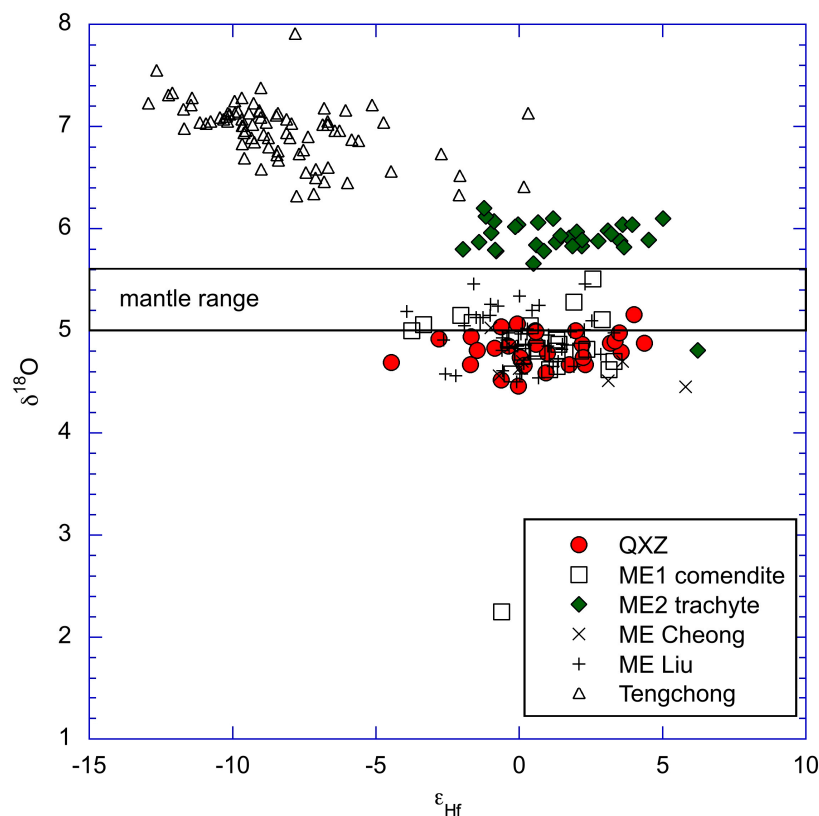


Figure 8. Comparison of Changbaishan zircon Hf–O with Tengchong zircon Hf–O isotopes. Tengchong zircons [14,15] show negative Hf–O isotope correlations whereas Changbaishan zircons show no significant correlations.

5. Conclusions

1. Zircons from pre-caldera QXZ comendites and syn-caldera ME1 comendites have $\delta^{18}\text{O}$ values lower than the mantle zircon values. If low- $\delta^{18}\text{O}$ zircons generally occur in caldera-forming eruptions, then a proto-caldera at Changbaishan might have formed before the QXZ eruption at 10 ka.
2. Zircons from ME2 trachytes have $\delta^{18}\text{O}$ values slightly higher than normal mantle values.
3. There are no correlations between zircon O and Hf isotopic compositions for QXZ, ME1, and ME2 zircons.
4. Shallow-level remelting produced the low- $\delta^{18}\text{O}$ zircon crystals in QXZ and ME1 peralkaline rhyolites.
5. ME2 trachytes with normal mantle values were not affected or assimilated by shallow-level remelting and were tapped from a deeper magma chamber.

Author Contributions: Conceptualization, H.Z.; methodology, H.Z. and J.T.; formal analysis, J.T. and H.Z.; investigation, J.T. and H.Z.; resources, H.Z.; data curation, H.Z. and J.T.; writing—original draft preparation, H.Z.; writing—review and editing, H.Z. and J.T.; visualization, H.Z.; supervision, H.Z.; project administration, H.Z.; funding acquisition, H.Z. All authors have read and agreed to the published version of the manuscript.

Funding: This research was funded by the National Natural Science Foundation of China, grant number 42230302.

Data Availability Statement: Data supporting reported results are given in Table 1.

Acknowledgments: We are grateful to Yongwei Zhao, Qicheng Fan, Liwen Chang, and Zipei Guo for their discussions and assistance.

Conflicts of Interest: The authors declare no conflicts of interest. The funders had no role in the design of the study; in the collection, analyses, or interpretation of data; in the writing of the manuscript; or in the decision to publish the results.

References

1. Zou, H.B.; Fan, Q.C.; Zhang, H.F. Rapid development of the great Millennium eruption of Changbaishan (Tianchi) Volcano: Evidence from U-Th zircon dating. *Lithos* **2010**, *119*, 289–296. [[CrossRef](#)]
2. Stone, R. Sizing up a slumbering giant. *Science* **2013**, *341*, 1060–1061. [[CrossRef](#)]
3. Lacovino, K.; Kim, J.S.; Sisson, T.; Lowenstern, J.B.; Ri, K.H.; Jang, J.N.; Song, K.H.; Ham, S.H.; Oppenhermer, C.; Hammond, J.O.S.; et al. Quantifying gas emissions from the “Millennium Eruption” of Paektu volcano, Democratic People’s Republic of Korea/China. *Sci. Adv.* **2016**, *2*, e1600913. [[CrossRef](#)] [[PubMed](#)]
4. Horn, S.; Schmincke, H.U. Volatile emission during the eruption of Baitoushan Volcano (China/North Korea) ca. 969 AD. *Bull. Volcanol.* **2000**, *61*, 537–555. [[CrossRef](#)]
5. Pan, B.; de Silva, S.L.; Xu, J.D.; Chen, Z.Q.; Miggins, D.P.; Wei, H.Q. The VEI-7 Millennium eruption, Changbaishan-Tianchi volcano, China/DPRK: New field, petrological, and chemical constraints on stratigraphy, volcanology, and magma dynamics. *J. Volcanol. Geotherm. Res.* **2017**, *343*, 45–59. [[CrossRef](#)]
6. Basu, A.R.; Wang, J.W.; Huang, W.K.; Xie, G.H.; Tatsumoto, M. Major element, REE, and Pb, Nd and Sr isotopic geochemistry of Cenozoic volcanic rocks of eastern China: Implications for their origin from suboceanic-type mantle reservoirs. *Earth Planet. Sci. Lett.* **1991**, *105*, 149–169. [[CrossRef](#)]
7. Zou, H.B.; Fan, Q.C.; Zhang, H.F.; Schmitt, A.K. U-series zircon age constraints on the plumbing system and magma residence times of the Changbai volcano, China/North Korea border. *Lithos* **2014**, *200–201*, 169–180. [[CrossRef](#)]
8. Channell, J.E.T.; Singer, B.S.; Jicha, B.R. Timing of Quaternary geomagnetic reversals and excursions in volcanic and sedimentary archives. *Quat. Sci. Rev.* **2020**, *228*, 106114. [[CrossRef](#)]
9. Wei, H.Q.; Liu, G.M.; Gill, J.B. Review of eruptive activity at Tianchi volcano, Changbaishan, northeast China: Implications for possible future eruptions. *Bull. Volcanol.* **2013**, *75*, 706. [[CrossRef](#)]
10. Zhao, D.P.; Yu, S.; Ohtani, E. East Asia: Seismotectonics, magmatism and mantle dynamics. *J. Asian Earth Sci.* **2011**, *40*, 689–709. [[CrossRef](#)]
11. Singer, B.S.; Jicha, B.R.; He, H.Y.; Zhu, R.X. Geomagnetic field excursion recorded 17 ka at Tianchi Volcano, China: New $^{40}\text{Ar}/^{39}\text{Ar}$ age and significance. *Geophys. Res. Lett.* **2014**, *41*, 2794–2802. [[CrossRef](#)]
12. Zou, H.B.; Vazquez, J.A.; Zhao, Y.W.; Guo, Z.P. Zircon surface crystallization ages for the extremely reduced magmatic products of the Millennium Eruption, Changbaishan Volcano (China/North Korea). *Gondwana Res.* **2021**, *92*, 172–183. [[CrossRef](#)]
13. Cheong, A.C.; Jeong, Y.J.; Jo, H.J.; Sohn, Y.K. Recurrent Quaternary magma generation at Baekdusan (Changbaishan) volcano: New zircon U-Th ages and Hf isotopic constraints from the Millennium Eruption. *Gondwana Res.* **2019**, *68*, 13–21. [[CrossRef](#)]
14. Guo, Z.P.; Zou, H.B. Temperature and Hf-O isotope correlations of young erupted zircons from Tengchong (SE Tibet): Assimilation fractional crystallization during monotonic cooling. *Geosci. Front.* **2023**, *14*, 101497. [[CrossRef](#)]
15. Tong, J.; Zou, H.B.; Guo, Z.P.; Chang, L.W.; Wang, L.Z.; Zhao, Y.W. Geochronology and Origin of Quaternary Dacites from the Daliuchong Volcano in the Tengchong Volcanic Field (TVF), SE Tibetan Plateau. *Minerals* **2024**, *14*, 990. [[CrossRef](#)]
16. Hawkesworth, C.J.; Kemp, A.I.S. Using hafnium and oxygen isotopes in zircons to unravel the record of crustal evolution. *Chem. Geol.* **2006**, *226*, 144–162. [[CrossRef](#)]
17. Choi, H.O.; Oh, J.; Kim, C.H.; Choi, S.Y.; Kim, W.H.; Park, C.H. Zircon U-Pb ages and O-Hf isotopes of Quaternary trachytes from the East Sea: Implications for the genesis of low- $\delta^{18}\text{O}$ magmas. *Geosci. Front.* **2024**, *15*, 101738. [[CrossRef](#)]
18. Lan, Z.W.; Pandey, S.K.; Zhang, S.J.; Sharma, M.; Gao, Y.Y.; Wu, S.T. Precambrian crustal evolution in Northern Indian Block: Evidence from detrital zircon U-Pb ages and Hf-isotopes. *Precambrian Res.* **2021**, *361*, 106238. [[CrossRef](#)]
19. Cheong, A.C.; Sohn, Y.K.; Jeong, Y.J.; Jo, H.J.; Park, K.H.; Lee, Y.S.; Li, X.H. Latest Pleistocene crustal cannibalization at Baekdusan (Changbaishan) as traced by oxygen isotopes of zircons from the Millennium Eruption. *Lithos* **2017**, *284–285*, 132–137. [[CrossRef](#)]
20. Liu, Y.J.; Zhang, C.; Xu, H.; Chen, L.H.; Pan, B. Recycled Oceanic Crust in the Source of the Intraplate Changbaishan-Tianchi Volcano, China/North Korea. *Geochem. Geophys. Geosystems* **2024**, *25*, e2024GC011764. [[CrossRef](#)]
21. Machida, H.; Arai, F. Extensive ash falls in and around the Sea of Japan from large late Quaternary eruptions. *J. Volcanol. Geotherm. Res.* **1983**, *18*, 151–164. [[CrossRef](#)]
22. Zou, H.B.; Tong, J.; Guo, Z.P. Young zircon Hf-O isotope constraints on the dynamics of magmatic reservoirs below Changbai (Paektu) volcano, China/North Korea. In Proceedings of the Goldschmidt Conference, Lyon, France, 9–14 July 2023. [[CrossRef](#)]
23. Li, X.H.; Li, W.X.; Li, Q.L.; Wang, X.C.; Liu, Y.; Yang, Y.H. Petrogenesis and tectonic significance of the ~850 Ma Gangbian alkaline complex in South China: Evidence from in situ zircon U-Pb dating, Hf-O isotopes and whole-rock geochemistry. *Lithos* **2010**, *114*, 1–15. [[CrossRef](#)]

24. Li, X.H.; Long, W.G.; Li, Q.L.; Zheng, Y.F.; Yang, Y.H.; Chamberlain, K.R.; Wan, D.F.; Guo, C.H.; Wang, X.C.; Tao, H. Penglai zircon megacrysts: A potential new working reference material for microbeam determination of Hf-O isotopes and U-Pb Age. *Geostand. Geoanalytical Res.* **2010**, *34*, 117–134. [[CrossRef](#)]
25. Hou, K.J.; Li, Y.H.; Zou, T.R.; Qu, X.M.; Shi, Y.R.; Xie, G.Q. Laser ablation-MC-ICP-MS technique for Hf isotope microanalysis of zircon and its geological applications. *Acta Petrol. Sin.* **2007**, *23*, 2595–2604.
26. Blichert-Toft, J.; Albarede, F. The Lu-Hf isotope geochemistry of chondrites and the evolution of the mantle-crust system. *Earth Planet. Sci. Lett.* **1997**, *148*, 243–258. [[CrossRef](#)]
27. Valley, J.W.; Kinny, P.D.; Schulze, D.J.; Spicuzza, M.J. Zircon megacrysts from kimberlite: Oxygen isotope variability among mantle melts. *Contrib. Mineral. Petrol.* **1998**, *131*, 1–11. [[CrossRef](#)]
28. Bindeman, I.N.; Valley, J.W. Low- $\delta^{18}\text{O}$ rhyolites from Yellowstone: Magmatic evolution based on analyses of zircons and individual phenocrysts. *J. Petrol.* **2001**, *42*, 1491–1517. [[CrossRef](#)]
29. Troch, J.; Ellis, B.S.; Harris, C.; Ulmer, P.; Bouvier, A.S.; Bachmann, O. Experimental Melting of Hydrothermally Altered Rocks: Constraints for the Generation of Low- $\delta^{18}\text{O}$ Rhyolites in the Central Snake River Plain. *J. Petrol.* **2019**, *60*, 1881–1902. [[CrossRef](#)]
30. Bindeman, I.N.; Schmitt, A.K.; Valley, J.W. U-Pb zircon geochronology of silicic tuffs from the Timber Mountain/Oasis Valley caldera complex, Nevada: Rapid generation of large volume magmas by shallow-level remelting. *Contrib. Mineral. Petrol.* **2006**, *152*, 649–665. [[CrossRef](#)]
31. Lan, Z.W.; Li, X.H.; Zhang, Q.R.; Li, Q.L. Global synchronous initiation of the 2nd episode of Sturtian glaciation: SIMS zircon U-Pb and O isotope evidence from the Jiangkou Group, South China. *Precambrian Res.* **2015**, *267*, 28–38. [[CrossRef](#)]
32. Wang, X.C.; Li, Z.X.; Li, X.H.; Li, Q.L.; Tang, G.Q.; Zhang, Q.R.; Liu, Y. Nonglacial origin for low- $\delta^{18}\text{O}$ Neoproterozoic magmas in the South China Block: Evidence from new in-situ oxygen isotope analyses using SIMS. *Geology* **2011**, *39*, 735–738. [[CrossRef](#)]
33. Hammond, J.O.S.; Wu, J.P.; Ri, K.S.; Wei, W.; Yu, J.N.; Oppenheimer, C. Distribution of Partial Melt Beneath Changbaishan/Paektu Volcano, China/Democratic People's Republic of Korea. *Geochem. Geophys. Geosystems* **2020**, *21*, e2019GC008461. [[CrossRef](#)]
34. Chou, G.G.; Fei, F.G.; Fang, H.; Du, B.R.; Zhang, X.B.; Zhang, P.H.; Yuan, Y.Z.; He, M.X.; Bai, D.W. Analysis of magma chamber at the Tianchi volcano area in Changbai mountain. *Chin. J. Geophys.* **2014**, *57*, 3466–3477.
35. Xu, J.D.; Liu, G.M.; Wu, J.P.; Ming, Y.H.; Wang, Q.L.; Cui, D.X.; Shangguan, Z.G.; Pan, B.; Lin, X.D.; Liu, J.Q. Recent unrest of Changbaishan volcano, northeast China: A precursor of a future eruption? *Geophys. Res. Lett.* **2012**, *39*, L16305. [[CrossRef](#)]
36. Zhang, M.L.; Guo, Z.F.; Liu, J.Q.; Liu, G.M.; Zhang, L.H.; Lei, M.; Zhao, W.B.; Ma, L.; Sepe, V.; Ventura, G. The intraplate Changbaishan volcanic field (China/North Korea): A review on eruptive history, magma genesis, geodynamic significance, recent dynamics and potential hazards. *Earth-Sci. Rev.* **2018**, *187*, 19–52. [[CrossRef](#)]
37. Yan, D.; Tian, Y.; Zhao, D.P.; Li, H.L. Seismicity and Magmatic System of the Changbaishan Intraplate Volcano in East Asia. *J. Geophys. Res. Solid Earth* **2023**, *128*, e2023JB026853. [[CrossRef](#)]
38. Zheng, Y.F.; Wu, Y.B.; Chen, F.K.; Gong, B.; Li, L.; Zhao, Z.F. Zircon U-Pb and oxygen isotope evidence for a large-scale ^{18}O depletion event in igneous rocks during the Neoproterozoic. *Geochim. Cosmochim. Acta* **2004**, *68*, 21. [[CrossRef](#)]
39. Bindeman, I. Oxygen isotopes in mantle and crustal magmas as revealed by single crystal analysis. *Rev. Mineral. Geochem.* **2008**, *69*, 445–478. [[CrossRef](#)]
40. Troch, J.; Ellis, B.S.; Harris, C.; Bachmann, O.; Bindeman, I.N. Low- $\delta^{18}\text{O}$ silicic magmas on Earth: A review. *Earth-Sci. Rev.* **2020**, *208*, 103299. [[CrossRef](#)]
41. Li, X.H.; Faure, M.; Lin, W.; Manatschal, G. New isotopic constraints on age and magma genesis of an embryonic oceanic crust. *Lithos* **2013**, *160–161*, 283–291. [[CrossRef](#)]
42. Zou, H.B.; Fan, Q.C.; Yao, Y.P. U-Th systematics of dispersed young volcanoes in NE China: Asthenosphere upwelling caused by piling up and upward thickening of stagnant Pacific slab. *Chem. Geol.* **2008**, *255*, 134–142. [[CrossRef](#)]

Disclaimer/Publisher's Note: The statements, opinions and data contained in all publications are solely those of the individual author(s) and contributor(s) and not of MDPI and/or the editor(s). MDPI and/or the editor(s) disclaim responsibility for any injury to people or property resulting from any ideas, methods, instructions or products referred to in the content.